medRxiv preprint doi: https://doi.org/10.1101/2020.01.24.20018697; this version posted January 28, 2020. The copyright holder for this preprint (which was not certified by peer review) is the author/funder, who has granted medRxiv a license to display the preprint in perpetuity. It is made available under a CC-BY-NC-ND 4.0 International license .

Reduced synaptic density in progressive supranuclear palsy and corticobasal syndrome, revealed by [^{11}C]UCB-J PET.

Negin Holland (MRCP)[1], P. Simon Jones (MSc)[1], George Savulich (PhD)[2], Julie K. Wiggins[1], Young T. Hong (PhD)[3], Tim D. Fryer (PhD)[3], Roido Manavaki (PhD) [4], Selena Milicevic-Sephton (PhD)[3], Istvan Boros (PhD)[1,3], Frank H. Hezemans (MSc)[1,6], Franklin I. Aigbirhio (DPhil)[1] , Jonathan P. Coles (FRCA, PhD)[5,7], John O'Brien (FRCP, PhD)[2,7], James B. Rowe (FRCP, PhD)[1,6,7].

1- Department of Clinical Neurosciences, University of Cambridge
2- Department of Psychiatry, University of Cambridge
3- Wolfson Brain Imaging Centre, University of Cambridge
4- Department of Radiology, University of Cambridge
5- Division of Anaesthesia, Department of Medicine, University of Cambridge
6- Medical Research Council Cognition and Brain Sciences Unit, University of Cambridge
7- Cambridge University Hospitals NHS Foundation Trust, Cambridge, UK

Correspondence to:

Dr Negin Holland

Department of Clinical Neuroscience, University of Cambridge, CB2, 0SZ, UK

Email: nda26@medschl.cam.ac.uk

NOTE: This preprint reports new research that has not been certified by peer review and should not be used to guide clinical practice.

medRxiv preprint doi: https://doi.org/10.1101/2020.01.24.20018697; this version posted January 28, 2020. The copyright holder for this preprint (which was not certified by peer review) is the author/funder, who has granted medRxiv a license to display the preprint in perpetuity. It is made available under a CC-BY-NC-ND 4.0 International license .

Abstract

Synaptic loss is prominent in several human neurodegenerative diseases. We tested the hypothesis that synaptic density is reduced by the primary tauopathies of progressive supranuclear palsy (PSP-Richardson's syndrome) and corticobasal syndrome (CBS). Thirty-seven participants (12 CBS, 10 PSP, and 15 age-/sex-/education-matched controls) underwent clinical and neuropsychological assessment, 3T magnetic resonance imaging, and positron emission tomography with the radioligand [^{11}C]UCB-J which targets the Synaptic Vesicle Glycoprotein 2A (SV2A). 10 CBS patients had negative β-amyloid biomarkers (Pittsburgh Compound B PET). As expected, patients with PSP-Richardson's syndrome and amyloid-negative CBS were impaired in executive, memory and visuospatial tasks. [^{11}C]UCB-J binding was reduced across frontal, temporal, parietal, and occipital lobes, cingulate, hippocampus, insula, amygdala and subcortical structures in both PSP and CBS patients compared to controls ($p<0.001$), with reductions up to 50%, consistent with post mortem data. The revised Addenbrooke's Cognitive Examination score correlated positively with [^{11}C]UCB-J binding in frontal, temporal, parietal, occipital, and cingulate cortices, as well as in the hippocampus, insula and amygdala, $p<0.05$); putamen and frontal lobe [^{11}C]UCB-J binding correlated inversely with the PSP rating scale ($p<0.05$). In conclusion, we confirm severe synaptic loss in PSP and CBS, which correlates with disease severity, providing critical insights into the underlying pathophysiology of primary degenerative tauopathies and supporting potential treatment strategies based on synaptic maintenance or restoration.

Keywords: Synaptic Vesicle Protein 2A, UCB-J, PET, tauopathy, PSP.

Abbreviations: [^{11}C]UCBJ = (*R*)-1-((3-(methyl-11C)pyridin-4-yl)methyl)-4-(3,4,5-trifluorophenyl)pyr-rolidin-2-one); BP_{ND} = non-displaceable binding potential; PSP = Progressive Supranuclear Palsy, CBS = corticobasal syndrome, CBD = Corticobasal Degeneration; [^{11}C]PiB = (methyl-11C) Pittsburgh compound B; UPDRS = Unified Parkinson's Disease Rating Scale; PSPRS = Progressive Supranuclear Gaze Palsy Rating Scale; ACE-R = Addenbrooke's Cognitive Examination – Revised; MMSE = Mini-mental State Examination; CDR = Clinical Dementia Rating Scale; CBI = Cambridge Behavioural Inventory – Revised; SEADL = Schwab and England Activities of Daily Living Scale. ns = non-significant at $p<0.05$.

medRxiv preprint doi: https://doi.org/10.1101/2020.01.24.20018697; this version posted January 28, 2020. The copyright holder for this preprint (which was not certified by peer review) is the author/funder, who has granted medRxiv a license to display the preprint in perpetuity. It is made available under a CC-BY-NC-ND 4.0 International license .

Introduction

The primary degenerative tauopathies of Progressive Supranuclear Palsy (PSP) and Corticobasal Degeneration (CBD) cause a severe combination of movement and cognitive impairment (Litvan *et al.*, 1996; Armstrong *et al.*, 2013; Burrell *et al.*, 2014; Höglinger *et al.*, 2017). Pathologically both are associated with a 4-repeat tauopathy; the underlying pathology of the clinical Corticobasal syndrome CBS is heterogeneous with corticobasal degeneration forming the majority and Alzheimer's disease pathology forming a substantial minority (Alexander *et al.*, 2014). Both PSP and CBD are associated with cortical and subcortical atrophy on magnetic resonance imaging (MRI) (Jabbari *et al.*, 2019); as well as changes in spatiotemporal features of neurophysiology and connectivity measured by magnetoencephalography and functional MRI (Hughes *et al.*, 2014; Wolpe *et al.*, 2014; Cope *et al.*, 2018; Sami *et al.*, 2018).

We proposed that the neurophysiological and connectivity impairments are a consequence of the loss of synapses. For example, at *post mortem* there is approximately 50% loss of cortical synapses in PSP and CBD (Bigio *et al.*, 2001; Lipton *et al.*, 2001). Transgenic models of tauopathies (e.g. rTg4510) confirm a synaptotoxic effect of oligomeric tau, before cell death (Menkes-Caspi *et al.*, 2015; Kaniyappan *et al.*, 2017). Moreover, in other neurodegenerative dementias, such as Alzheimer's disease, synaptic loss correlates better with cognitive dysfunction than atrophy (Terry *et al.*, 1991).

We therefore tested whether PSP and CBD reduce synaptic plasticity *in vivo*, and in proportion to disease severity. We used positron emission tomography (PET) with the radioligand ((*R*)-1-((3-(methyl-11C)pyridin-4-yl)methyl)-4-(3,4,5-trifluorophenyl)pyrrolidin-2-one), known as [^{11}C]UCB-J, manufactured at the Wolfson Brain Imaging Centre Radiopharmaceutical Unit (Milicevic Sephton *et al.*, 2020). This ligand quantifies synaptic density (Finnema *et al.*, 2016, 2017) based on its affinity for the presynaptic vesicle glycoprotein 2A (SV2a), that is ubiquitously expressed in brain synapses (Bajjalieh *et al.*, 1993, 1994). [^{11}C]UCB-J has revealed hippocampal synaptic loss in Alzheimer's disease, correlating with episodic memory loss and clinical dementia severity (Chen *et al.*, 2018). We use β-amyloid biomarkers to identify which cases of CBS are likely to not be caused by Alzheimer's disease pathology (Alexander *et al.*, 2014) and are tentatively considered to have CBD. We sought correlations between regional [^{11}C]UCB-J binding potential, a metric of

medRxiv preprint doi: https://doi.org/10.1101/2020.01.24.20018697; this version posted January 28, 2020. The copyright holder for this preprint (which was not certified by peer review) is the author/funder, who has granted medRxiv a license to display the preprint in perpetuity. It is made available under a CC-BY-NC-ND 4.0 International license .

SV2A (synaptic) density, and disease severity, in terms of cognitive decline and measures of global impairment.

medRxiv preprint doi: https://doi.org/10.1101/2020.01.24.20018697; this version posted January 28, 2020. The copyright holder for this preprint (which was not certified by peer review) is the author/funder, who has granted medRxiv a license to display the preprint in perpetuity. It is made available under a CC-BY-NC-ND 4.0 International license .

Materials & Methods

Participants & Study Design

Patients were recruited from a tertiary specialist clinic for PSP/CBS. Healthy volunteers were recruited from the UK National Institute for Health Research Join Dementia Research (JDR) register. Patients had either probable PSP–Richardson Syndrome (Höglinger *et al.*, 2017), or both probable CBS and probable CBD (Armstrong *et al.*, 2013). Participants underwent a clinical and cognitive assessment including measures of disease severity (Table 1), 3T MRI, and [^{11}C]UCB-J PET.

Patients with CBS underwent amyloid PET imaging using carbon 11-Pittsburgh Compound B ([^{11}C]PiB). Only those with a negative amyloid status as characterised by a [^{11}C]PiB standardised uptake value ratio (SUVR; 50-70 minutes post injection; whole cerebellum reference tissue) less than 1.21 (Centiloid scale 19; (Jack *et al.*, 2017)) are included in the subsequent analysis, with the aim of excluding patients with CBS due to Alzheimer's disease. We interpret this amyloid-negative group as having CBD, although acknowledge that other pathologies are possible.

The research protocol was approved by the local Cambridge Research Ethics Committee and the Administration of Radioactive Substances Advisory Committee. All participants provided written informed consent in accordance with the Declaration of Helsinki.

Neuroimaging

Dynamic PET data acquisition was performed on a GE SIGNA PET/MR (GE Healthcare, Waukesha, USA) for 90 minutes starting immediately after [^{11}C]UCB-J injection (median injected activity: 351 ± 107 MBq, injected mass ≤ 10 μg), with attenuation correction including the use of a multi-subject atlas method (Burgos *et al.*, 2014; Prados *et al.*, 2016) and also improvements to the MRI brain coil component (Manavaki *et al.*, 2019). Each emission image series was aligned using SPM12 (www.fil.ion.ucl.ac.uk/spm/software/spm12/) then rigidly registered to a T1-weighted MRI acquired during PET data acquisition (TR = 3.6 msec, TE = 9.2 msec, 192 sagittal slices, in plane resolution 0.55 x 0.55 mm (subsequently interpolated to 1.0 x 1.0 mm); slice thickness 1.0 mm). Using a modified Hammersmith atlas with subcortical regions (http://brain-development.org), combined regions of interest (in frontal, parietal, occipital, and temporal

medRxiv preprint doi: https://doi.org/10.1101/2020.01.24.20018697; this version posted January 28, 2020. The copyright holder for this preprint (which was not certified by peer review) is the author/funder, who has granted medRxiv a license to display the preprint in perpetuity. It is made available under a CC-BY-NC-ND 4.0 International license .

lobes; cingulate, and cerebellum) were spatially normalized to the T1-weighted MRI of each participant using ANTs software (Avants *et al.*, 2008), then multiplied by a grey matter binary mask (>50% grey matter on the SPM12 probability map, smoothed to PET spatial resolution). Regional time-activity curves were extracted with and without correction for cerebrospinal fluid (CSF) partial volume using the SPM12 CSF probability map, again smoothed to PET resolution. To quantify SV2A density, [^{11}C]UCB-J non-displaceable binding potential (BP_{ND}) was determined using a basis function implementation of the simplified reference tissue model (Wu and Carson, 2002), with the reference tissue defined in the centrum semiovale (Koole *et al.*, 2019; Rossano *et al.*, 2019). Group average BP_{ND} images (illustrated in Fig1 A-C) were obtained by spatially normalizing individual T1-weighted MRI (and thereby co-registered BP_{ND} map) to MNI space, and then to the group template using ANTS.

Statistical analysis

Statistical analyses used R (version 3.6.2), with analysis of covariance (ANCOVA) to compare regional [^{11}C]UCB-J BP_{ND} between the three groups (Control, CBD, PSP), with age as a covariate of no interest. Regions of interest were: frontal, temporal, parietal, occipital lobes, cingulate cortex, hippocampus, insula, amygdala, putamen, thalamus, cerebellum, and midbrain.

The relationships between [^{11}C]UCB-J BP_{ND}, disease severity (PSP Rating Scale) and cognition (revised Addenbrooke's Cognitive Examination) were tested through linear models of the patient data, with age as a covariate of no interest. All analyses were repeated using CSF uncorrected BP_{ND}.

Data availability

The derived data that support the findings of this study are available from the corresponding author, upon reasonable request for academic (non-commercial) purposes.

medRxiv preprint doi: https://doi.org/10.1101/2020.01.24.20018697; this version posted January 28, 2020. The copyright holder for this preprint (which was not certified by peer review) is the author/funder, who has granted medRxiv a license to display the preprint in perpetuity. It is made available under a CC-BY-NC-ND 4.0 International license .

Results

Of the twelve patients with CBS, two had PiB SUVR ratios of 2.32 and 1.61 and were therefore excluded from further analysis. The remaining groups (ten CBD, ten PSP, fifteen controls) were matched in age, gender and education (Table 1). We observed typical cognitive profiles, as summarised in Table 1: patients were impaired on memory, verbal fluency, language and visuospatial domains of the ACE-revised, Mini-Mental State Examination and Montreal Cognitive Assessment. There were high endorsements on the Cambridge Behavioural Inventory, and the Clinical Dementia Rating scale, with impairment of activities of daily living on the Schwab and England scale.

The average BP_{ND} map per group is illustrated in Fig.1A-C, alongside a scatter plot of individual regional BP_{ND} values for all participants (Fig. 1D). Regional CSF-corrected BP_{ND} values for the three groups are shown in Table 2. There was a widespread reduction in [^{11}C]UCB-J BP_{ND} in frontal, temporal, parietal, occipital, and cingulate cortex, cerebellum, thalamus, insula, amygdala, caudate nucleus, putamen, and midbrain ($p<0.05$ FDR corrected). BP_{ND} in PSP and CBD was 30-50% lower than controls, with the most severe median reductions in the midbrain and frontal and parietal lobes of patients with PSP and in the hippocampus, cerebellum and caudate nucleus of patients with CBD. The same pattern of significant reductions in BP_{ND} was observed using CSF-uncorrected data.

Correlations between [^{11}C]UCB-J BP_{ND}, the PSP rating scale and cognition in patients are given in Fig. 2. There were positive correlations between ACE-R and BP_{ND} in widespread cortical and subcortical regions (Fig. 2A; frontal lobe R^2 =0.38, p= 0.04; temporal lobe R^2 = 0.41, p=0.04; parietal lobe R^2 = 0.45, p=0.04; occipital lobe R^2 =0.40, p=0.04; insula R^2 = 0.41, p=0.04; cingulate cortex R^2 =0.40, p=0.04; and hippocampus R^2 =0.35, p=0.05; FDR corrected). An inverse correlation was observed between the PSP rating scale and BP_{ND} in the frontal lobe R^2 =0.39, p= 0.05, and the putamen R^2=0.25, p=0.049 (FDR corrected; Fig. 2B). We also observed a negative correlation between [^{11}C]UCB-J BP_{ND} and the Cambridge Behavioral Inventory (marker of global impairment based on carers' rating) in the frontal lobe, R^2 =0.3, p=0.04 (uncorrected). Except for the latter, similar correlations were observed using CSF uncorrected data.

medRxiv preprint doi: https://doi.org/10.1101/2020.01.24.20018697; this version posted January 28, 2020. The copyright holder for this preprint (which was not certified by peer review) is the author/funder, who has granted medRxiv a license to display the preprint in perpetuity. It is made available under a CC-BY-NC-ND 4.0 International license .

Discussion

The principal result of this study is to confirm a severe reduction in synaptic density in PSP-Richardson's syndrome and amyloid-negative CBS. This accords with *post mortem* estimates of PSP and CBD, using synaptophysin immunohistochemistry, and morphological studies of cortical dendrites in the closely related condition of frontotemporal lobe dementia (Ferrer *et al.*, 1991; Bigio *et al.*, 2001). Indirect evidence of synaptic loss, from consequential reduction in metabolism, comes from [^{18}F]FDG PET changes in frontal, temporal and parietal lobes (Foster *et al.*, 1988; Eidelberg *et al.*, 1991; Blin *et al.*, 1992; Juh *et al.*, 2004). However, PET imaging with ligand [^{11}C]UCB-J provides direct evidence *in vivo* of severe and extensive loss of cortical and subcortical synapses, including areas of the brain that are minimally atrophic (Josephs *et al.*, 2008).

Progressive supranuclear palsy and corticobasal degeneration are progressive, with an average disease duration of five to eight years from symptom onset (Coyle-Gilchrist *et al.*, 2016). In our clinically diagnosed CBD and PSP groups, the mean symptom duration at the time of PET was three and a half years, and with a pre-symptomatic period, we infer that our patients were likely to be over half-way through their disease course. The median reduction of 20% (and maximal 50%) in [^{11}C]UCB-J binding observed *in vivo* (compared to controls), is in keeping with the predictions from *post mortem* data. Interestingly, the cerebellum was markedly abnormal in CBD. Although cerebellar atrophy is not a typical association of CBS/CBD (Dickson *et al.*, 2007), we suggest this may represent cerebellar diaschisis in response to widespread cortical pathology and loss of cortico-cerebellar projections.

Preclinical models of tauopathy suggest early synaptotoxicity with reduced plasticity and density (Menkes-Caspi *et al.*, 2015), in response to soluble oligomeric tau aggregates (Kaniyappan *et al.*, 2017) and inflammation (Rajendran and Paolicelli, 2018). The toxicity associated with tau pathology leading to synapse loss is complex and involves direct and indirect pathways (reviewed in (Spires-Jones and Hyman, 2014). Naturally occurring tau plays a role in synaptic function through modulating microtubule and axonal stability; disruptions to this machinery leads to prevention of the trafficking of essential components to synapses such as synaptic receptors (Hoover *et al.*, 2010) and mitochondria. Indeed, over-expression of tau interferes with mitochondria transport (Stoothoff *et al.*, 2009), and

medRxiv preprint doi: https://doi.org/10.1101/2020.01.24.20018697; this version posted January 28, 2020. The copyright holder for this preprint (which was not certified by peer review) is the author/funder, who has granted medRxiv a license to display the preprint in perpetuity. It is made available under a CC-BY-NC-ND 4.0 International license .

contributes to hyperexcitability of neurons and impaired calcium influx in transgenic mouse models (rTg4510) (Rocher *et al.*, 2010).

Here we observe a significant correlation between synaptic loss and disease severity both in the context of cognitive impairment and physical disability in PSP and CBD. Synaptic loss correlates with cognitive impairment in another clinical tauopathy, Alzheimer's disease (Terry *et al.*, 1991; Robinson *et al.*, 2014), and preclinical models of this (Walsh *et al.*, 2002; Kandimalla *et al.*, 2018). Our in vivo PET results support the potential use of synaptic PET as a marker of disease and progression, but longitudinal data are required. Synaptic PET may support early stage clinical trials in PSP and CBS/CBD; it is encouraging in this latter respect that UCB-J is sensitive to changes in synaptic density in response to treatment with the synaptic modulator Saracatinib (Toyonaga *et al.*, 2019).

Our study has several limitations. Although the sample size is small, it is adequately powered in view of the large effect sizes predicted. However, subtler relationships with mild disease, progression or individual clinical features, or phenotypic variants of PSP and CBS, require larger studies. We acknowledge the potential for off-target binding, but preclinical data indicate very high correlations between UCB-J and synaptophysin, a marker of synaptic vesicular density (Finnema *et al.*, 2016). Our diagnoses were clinical, without neuropathology, although the clinicopathological correlations of PSP-Richardson syndrome are very high, and in the absence of Alzheimer's disease, the clinicopathological correlation of CBS with a 4R-tauopathy (CBD or PSP) is similarly very high (Alexander *et al.*, 2014).

Early stage trials will require early accurate diagnosis, although diagnosis is typically made 3 years after symptom onset (Coyle-Gilchrist *et al.*, 2016; Mamarabadi *et al.*, 2018). It is unlikely that synaptic PET could provide pre-symptomatic diagnosis in rare conditions, but it is a promising tool to characterise pathogenetic mechanisms, monitor progression and assess the response to experimental medicines (Cai *et al.*, 2019).

medRxiv preprint doi: https://doi.org/10.1101/2020.01.24.20018697; this version posted January 28, 2020. The copyright holder for this preprint (which was not certified by peer review) is the author/funder, who has granted medRxiv a license to display the preprint in perpetuity. It is made available under a CC-BY-NC-ND 4.0 International license .

Acknowledgements

The authors would like to thank the participants, the staff at the Wolfson Brain Imaging Centre, and the staff at the Cambridge Centre for Parkinson-Plus.

Funding

The study was funded by the Cambridge University Centre for Parkinson-Plus; the National Institute for Health Research Cambridge Biomedical Research Centre (SUAG/004 RG91365 JBR); the Wellcome Trust (103838) and the Association of British Neurologists, Patrick Berthoud Charitable Trust (RG99368).

Competing interests

JBR serves as an associate editor to Brain, and is a non-remunerated trustee of the Guarantors of Brain and the PSP Association (UK). He provides consultancy to Asceneuron, Biogen, UCB and has research grants from AZ-Medimmune, Janssen, Lilly as industry partners in the Dementias Platform UK.

Supplementary Materials

Nil.

Legends

Figure 1:

(A-C) – Mean [^{11}C]UCB-J binding potential (BP_{ND}) maps (in axial, coronal and sagittal slices) for control participants (A), patients with CBD (B), and PSP (C).

(D) Scatter plot of individual regional [^{11}C]UCB-J binding potentials (BP_{ND}) values for control, CBD and PSP participants.

Figure 2:

(A) Correlations between total ACE-R score and regional [^{11}C]UCB-J binding potential (BP_{ND}) for the two patient groups.

medRxiv preprint doi: https://doi.org/10.1101/2020.01.24.20018697; this version posted January 28, 2020. The copyright holder for this preprint (which was not certified by peer review) is the author/funder, who has granted medRxiv a license to display the preprint in perpetuity. It is made available under a CC-BY-NC-ND 4.0 International license .

(B) Correlations between total PSP rating scale (PSPRS_total) and regional [^{11}C]UCB-J binding potential (BP_{ND}) in the frontal lobe and putamen for the two patient groups.

medRxiv preprint doi: https://doi.org/10.1101/2020.01.24.20018697; this version posted January 28, 2020. The copyright holder for this preprint (which was not certified by peer review) is the author/funder, who has granted medRxiv a license to display the preprint in perpetuity. It is made available under a CC-BY-NC-ND 4.0 International license .

References

Alexander SK, Rittman T, Xuereb JH, Bak TH, Hodges JR, Rowe JB. Validation of the new consensus criteria for the diagnosis of corticobasal degeneration. J Neurol Neurosurg Psychiatry 2014; 85: 923–927.

Armstrong MJ, Litvan I, Lang AE, Bak TH, Bhatia KP, Borroni B, et al. Criteria for the diagnosis of corticobasal degeneration. Neurology 2013; 80: 496–503.

Avants BB, Epstein CL, Grossman M, Gee JC. Symmetric diffeomorphic image registration with cross-correlation: Evaluating automated labeling of elderly and neurodegenerative brain. Med Image Anal 2008

Bajjalieh SM, Frantz GD, Weimann JM, McConnell SK, Scheller RH. Differential expression of synaptic vesicle protein 2 (SV2) isoforms. J Neurosci 1994; 14: 5223–5235.

Bajjalieh SM, Peterson K, Linial M, Scheller RH. Brain contains two forms of synaptic vesicle protein 2 [Internet]. 1993[cited 2019 Jun 26] Available from: https://www.ncbi.nlm.nih.gov/pmc/articles/PMC46043/pdf/pnas01465-0061.pdf

Bigio EH, Vono MB, Satumtira S, Adamson J, Sontag E, Hynan LS, et al. Cortical synapse loss in progressive supranuclear palsy. J Neuropathol Exp Neurol 2001; 60: 403–410.

Blin J, Vidailhet M-J, Pillon B, Dubois B, Feve J-R, Agid Y. Corticobasal degeneration: Decreased and asymmetrical glucose consumption as studied with PET. Mov Disord 1992; 7: 348–354.

Burgos N, Cardoso MJ, Thielemans K, Modat M, Pedemonte S, Dickson J, et al. Attenuation correction synthesis for hybrid PET-MR scanners: Application to brain studies. IEEE Trans Med Imaging 2014

Burrell JR, Hodges JR, Rowe JB. Cognition in corticobasal syndrome and progressive supranuclear palsy: A review. Mov Disord 2014; 29: 684–693.

Cai Z, Li S, Matuskey D, Nabulsi N, Huang Y. PET imaging of synaptic density: A new tool for investigation of neuropsychiatric diseases. Neurosci Lett 2019; 691: 44–50.

Chen MK, Mecca AP, Naganawa M, Finnema SJ, Toyonaga T, Lin SF, et al. Assessing Synaptic Density in Alzheimer Disease with Synaptic Vesicle Glycoprotein 2A Positron Emission Tomographic Imaging. JAMA Neurol 2018; 75: 1215–1224.

Cope TE, Rittman T, Borchert RJ, Jones PS, Vatansever D, Allinson K, et al. Tau burden and

medRxiv preprint doi: https://doi.org/10.1101/2020.01.24.20018697; this version posted January 28, 2020. The copyright holder for this preprint (which was not certified by peer review) is the author/funder, who has granted medRxiv a license to display the preprint in perpetuity. It is made available under a CC-BY-NC-ND 4.0 International license .

the functional connectome in Alzheimer's disease and progressive supranuclear palsy. Brain 2018; 141: 550–567.

Coyle-Gilchrist ITS, Dick KM, Patterson K, Rodríquez PV, Wehmann E, Wilcox A, et al. Prevalence, characteristics, and survival of frontotemporal lobar degeneration syndromes. Neurology 2016; 86: 1736–1743.

Dickson DW, Rademakers R, Hutton ML. Progressive Supranuclear Palsy: Pathology and Genetics. Brain Pathol 2007; 17: 74–82.

Eidelberg D, Dhawan V, Moeller JR, Sidtis JJ, Ginos JZ, Strother SC, et al. The metabolic landscape of cortico-basal ganglionic degeneration: regional asymmetries studied with positron emission tomography. Neurosurgery, and Psychiatry 1991; 54: 856–862.

Ferrer I, Roig C, Espino A, Peiro G, Matias Guiu X, Neuropatologia U, et al. Dementia of frontal lobe type and motor neuron disease. A Golgi study of the frontal cortex. 1991

Finnema SJ, Nabulsi NB, Eid T, Detyniecki K, Lin SF, Chen MK, et al. Imaging synaptic density in the living human brain [Internet]. Sci Transl Med 2016; 8[cited 2018 Nov 10] Available from: www.ScienceTranslationalMedicine.org

Finnema SJ, Nabulsi NB, Mercier J, Lin SF, Chen MK, Matuskey D, et al. Kinetic evaluation and test–retest reproducibility of [11C]UCB-J, a novel radioligand for positron emission tomography imaging of synaptic vesicle glycoprotein 2A in humans. J Cereb Blood Flow Metab 2017

Foster NL, Gilman S, Berent S, Morin EM, Brown MB, Koeppe RA. Cerebral hypometabolism in progressive supranuclear palsy studied with positron emission tomography. Ann Neurol 1988; 24: 399–406.

Höglinger GU, Respondek G, Stamelou M, Kurz C, Josephs KA, Lang AE, et al. Clinical diagnosis of progressive supranuclear palsy: The movement disorder society criteria. Mov Disord 2017; 32: 853–864.

Hoover BR, Reed MN, Su J, Penrod RD, Kotilinek LA, Grant MK, et al. Tau Mislocalization to Dendritic Spines Mediates Synaptic Dysfunction Independently of Neurodegeneration. Neuron 2010; 68: 1067–1081.

Hughes LE, Rowe JB, Ghosh BCP, Carlyon RP, Plack CJ, Gockel HE. The binaural masking level difference: Cortical correlates persist despite severe brain stem atrophy in progressive supranuclear palsy. J Neurophysiol 2014; 112: 3086–3094.

medRxiv preprint doi: https://doi.org/10.1101/2020.01.24.20018697; this version posted January 28, 2020. The copyright holder for this preprint (which was not certified by peer review) is the author/funder, who has granted medRxiv a license to display the preprint in perpetuity. It is made available under a CC-BY-NC-ND 4.0 International license .

Jabbari E, Holland N, Chelban V, Jones PS, Lamb R, Rawlinson C, et al. Diagnosis Across the Spectrum of Progressive Supranuclear Palsy and Corticobasal Syndrome. [Internet]. JAMA Neurol 2019[cited 2019 Dec 23] Available from: http://www.ncbi.nlm.nih.gov/pubmed/31860007

Jack CR, Wiste HJ, Weigand SD, Therneau TM, Lowe VJ, Knopman DS, et al. Defining imaging biomarker cut points for brain aging and Alzheimer's disease. Alzheimer's Dement 2017; 13: 205–216.

Josephs KA, Whitwell JL, Dickson DW, Boeve BF, Knopman DS, Petersen RC, et al. Voxel-based morphometry in autopsy proven PSP and CBD. Neurobiol Aging 2008; 29: 280–289.

Juh R, Kim J, Moon D, Choe B, Suh T. Different metabolic patterns analysis of Parkinsonism on the 18 F-FDG PET. Eur J Radiol 2004; 51: 223–233.

Kandimalla R, Manczak M, Yin X, Wang R, Reddy PH. Hippocampal phosphorylated tau induced cognitive decline, dendritic spine loss and mitochondrial abnormalities in a mouse model of Alzheimer's disease. Hum Mol Genet 2018; 27: 30–40.

Kaniyappan S, Chandupatla RR, Mandelkow EM, Mandelkow E. Extracellular low-n oligomers of tau cause selective synaptotoxicity without affecting cell viability. Alzheimer's Dement 2017; 13: 1270–1291.

Koole M, van Aalst J, Devrome M, Mertens N, Serdons K, Lacroix B, et al. Quantifying SV2A density and drug occupancy in the human brain using [11 C]UCB-J PET imaging and subcortical white matter as reference tissue. Eur J Nucl Med Mol Imaging 2019; 46: 396–406.

Lipton AM, Munro Cullum C, Satumtira S, Sontag E, Hynan LS, White CL, et al. Contribution of asymmetric synapse loss to lateralizing clinical deficits in frontotemporal dementias. Arch Neurol 2001; 58: 1233–1239.

Litvan I, Agid Y, Calne D, Campbell G, Dubois B, Duvoisin RC, et al. Clinical research criteria for the diagnosis of progressive supranuclear palsy (Steele-Richardson-Olszewski syndrome): Report of the NINDS-SPSP International Workshop. Neurology 1996; 47: 1–9.

Mamarabadi M, Razjouyan H, Golbe LI. Is the Latency from Progressive Supranuclear Palsy Onset to Diagnosis Improving? Mov Disord Clin Pract 2018; 5: 603–606.

Manavaki R, Hong Y, Fryer TD. Brain MRI coil attenuation map processing for the GE SIGNA PET/MR: Impact on PET image quantification and uniformity. IEEE Nucl Sci Symp

medRxiv preprint doi: https://doi.org/10.1101/2020.01.24.20018697; this version posted January 28, 2020. The copyright holder for this preprint (which was not certified by peer review) is the author/funder, who has granted medRxiv a license to display the preprint in perpetuity. It is made available under a CC-BY-NC-ND 4.0 International license .

Med Imaging Conf Proceedings 2019

Menkes-Caspi N, Yamin HG, Kellner V, Spires-Jones TL, Cohen D, Stern EA. Pathological tau disrupts ongoing network activity. Neuron 2015; 85: 959–966.

Milicevic Sephton S, Miklovicz T, Russell J, Doke A, Li L, Boros I. Automated radiosynthesis of [11C]UCB-J for imaging synaptic density by PET. J Label Compd Radiopharm 2020; In press.

Prados F, Cardoso MJ, Burgos N, Wheeler-Kingshott C, Ourselin S, Angela C, et al. NiftyWeb: web based platform for image processing on the cloud. In: 24th Scientific Meeting and Exhibition of the International Society for Magnetic Resonance in Medicine (ISMRM). 2016

Rajendran L, Paolicelli RC. Microglia-mediated synapse loss in Alzheimer's disease. J Neurosci 2018; 38: 2911–2919.

Robinson JL, Molina-Porcel L, Corrada MM, Raible K, Lee EB, Lee VMY, et al. Perforant path synaptic loss correlates with cognitive impairment and Alzheimer's disease in the oldest-old. Brain 2014; 137: 2578–2587.

Rocher AB, Crimins JL, Amatrudo JM, Kinson MS, Todd-Brown MA, Lewis J, et al. Structural and functional changes in tau mutant mice neurons are not linked to the presence of NFTs. Exp Neurol 2010; 223: 385–393.

Rossano S, Toyonaga T, Finnema SJ, Naganawa M, Lu Y, Nabulsi N, et al. Assessment of a white matter reference region for 11C-UCB-J PET quantification. J Cereb Blood Flow Metab 2019

Sami S, Williams N, Hughes LE, Cope TE, Rittman T, Coyle-Gilchrist ITS, et al. Neurophysiological signatures of Alzheimer's disease and frontotemporal lobar degeneration: Pathology versus phenotype. Brain 2018; 141: 2500–2510.

Spires-Jones TL, Hyman BT. The Intersection of Amyloid Beta and Tau at Synapses in Alzheimer's Disease. Neuron 2014; 82: 756–771.

Stoothoff W, Jones PB, Spires-Jones TL, Joyner D, Chhabra E, Bercury K, et al. Differential effect of three-repeat and four-repeat tau on mitochondrial axonal transport. J Neurochem 2009; 111: 417–427.

Terry RD, Masliah E, Salmon DP, Butters N, DeTeresa R, Hill R, et al. Physical basis of cognitive alterations in alzheimer's disease: Synapse loss is the major correlate of cognitive

medRxiv preprint doi: https://doi.org/10.1101/2020.01.24.20018697; this version posted January 28, 2020. The copyright holder for this preprint (which was not certified by peer review) is the author/funder, who has granted medRxiv a license to display the preprint in perpetuity. It is made available under a CC-BY-NC-ND 4.0 International license .

impairment. Ann Neurol 1991; 30: 572–580.

Toyonaga T, Smith LM, Finnema SJ, Gallezot J-D, Naganawa M, Bini J, et al. In vivo synaptic density imaging with 11 C-UCB-J detects treatment effects of saracatinib (AZD0530) in a mouse model of Alzheimer's disease. . J Nucl Med 2019: jnumed.118.223867.

Walsh DM, Klyubin I, Fadeeva J V., Cullen WK, Anwyl R, Wolfe MS, et al. Naturally secreted oligomers of amyloid β protein potently inhibit hippocampal long-term potentiation in vivo. Nature 2002; 416: 535–539.

Wolpe N, Moore JW, Rae CL, Rittman T, Altena E, Haggard P, et al. The medial frontal-prefrontal network for altered awareness and control of action in corticobasal syndrome. Brain 2014; 137: 208–220.

Wu Y, Carson RE. Noise reduction in the simplified reference tissue model for neuroreceptor functional imaging. J Cereb Blood Flow Metab 2002

medRxiv preprint doi: https://doi.org/10.1101/2020.01.24.20018697; this version posted January 28, 2020. The copyright holder for this preprint (which was not certified by peer review) is the author/funder, who has granted medRxiv a license to display the preprint in perpetuity. It is made available under a CC-BY-NC-ND 4.0 International license .

	Control	**CBD**	**PSP**	**F *(p)***
m:f	7:8	7:3	3:7	ns[a]
Age at scan	67.5 (7.4)	69.91 (8.13)	70.95 (8.6)	ns
Disease duration in years	NA	3.41 (1.55)	3.40 (1.38)	ns
Education in years	13.69 (2.66)	12.9 (3.11)	13.56 (6.44)	ns[b]
ACE_R total (max. 100)	96.47 (2.88)	85.4 (10.1)	77.60 (16.75)	8.26 (0.002)
Attention_Orientation (max .18)	17.87 (0.35)	17.3 (0.82)	16.30 (2.21)	4.54 (0.02)
Memory (max .26)	24.53 (1.85)	22.8 (3.68)	20.50 (4.03)	4.95 (0.01)
Fluency (max .14)	12.80 (1.15)	8.4 (2.76)	6.10 (3.7)	22.16 (0.000001)
Language (max .26)	25.53 (0.92)	23.2 (5.05)	22.70 (6.07)	ns
Visuospatial (max .16)	15.73 (0.59)	13.7 (2.58)	12.00 (4.4)	5.73 (0.007)
UPDRS (max. 132)	0(0)	37.4 (14.2)	30.00 (17.68)	36.59 (0.000)
PSPRS (max. 100)	0.13 (0.52)	26.9 (9.07)	29.40 (11.3)	57.12 (0.000)
CBDRS (max. 124)	0.20 (0.77)	26.7 (15.85)	37.11 (21.62)	22.68 (0.000)
MMSE (max. 30)	29.27 (1.33)	27.7 (1.57)	26.60 (2.99)	5.58 (0.008)
MoCA (max. 30)	27.80 (1.74)	14.33 (13.64)	20.40 (7.75)	7.93 (0.002)
Ineco (max. 30)	26.00 (1.85)	17.5 (9.59)	16.50 (5.24)	9.41 (0.001)
CDR sum of boxes (max. 32)	0.07 (0.26)	6.9 (4.38)	8.00 (7.18)	11.87 (0.0001)
CBI (max. 180)	2.47 (4.81)	26.7 (12.15)	53.00 (38.93)	16.15 (0.00001)
SEADL (max. 100)	99.23 (2.77)	61.43 (26.10)	58.57 (22.68)	17.19 (0.0001)

Table 1. Demographics and neuropsychological profile for each cohort of participants.

The results are given as mean (standard deviation). [a] chi-squared test. [b] ANOVA with PSP and CBD only. The F-statistic and p-values are derived from an ANCOVA with age as a covariate. UPDRS: Unified Parkinson's Disease Rating Scale, PSPRS: Progressive Supranuclear Palsy Rating Scale, ACE-R: revised Addenbrooke's Cognitive Examination, MMSE: Mini-mental State Examination, CDR: Clinical Dementia Rating Scale, CBI: revised Cambridge Behavioural Inventory, SEADL: Schwab and England Activities of Daily Living

medRxiv preprint doi: https://doi.org/10.1101/2020.01.24.20018697; this version posted January 28, 2020. The copyright holder for this preprint (which was not certified by peer review) is the author/funder, who has granted medRxiv a license to display the preprint in perpetuity. It is made available under a CC-BY-NC-ND 4.0 International license .

Scale. ns = non-significant at $p<0.05$; NA = non-applicable. CBD=corticobasal syndrome with evidence of the lack of significant B-amyloid pathology. PSP=PSP-Richardson's syndrome.

Table 2. Mean (standard deviation) CSF corrected [^{11}C]UCB-J BP_{ND} values per group for cortical and subcortical regions of interest with significant differences across groups (surviving false discovery rate correction over 13 regions).

Region	Control	CBD	PSP	F (p)
Hippocampus	2.22 (0.13)	1.8 (0.24)	1.82 (0.21)	17.00 (0.00001)
Insula	2.83 (0.15)	2.35 (0.25)	2.23 (0.26)	24.7 (0.00001)
Amygdala	2.61 (0.16)	2.12 (0.29)	2.14 (0.24)	16.51 (0.00001)
CaudateNucl	2.92 (0.17)	2.44 (0.38)	2.28 (0.31)	14.96 (0.00003)
Thalamus	2.63 (0.20)	2.21 (0.35)	2.07 (0.40)	9.72 (0.0005)
Putamen	3.39 (0.22)	2.88 (0.31)	2.71 (0.38)	17.25 (0.00001)
Midbrain	2.11 (0.15)	1.89 (0.30)	1.67 (0.33)	6.69 (0.004)
Frontal_lobe	3.26 (0.18)	2.76 (0.29)	2.50 (0.39)	22.34 (0.000001)
Temporal_lobe	2.82 (0.19)	2.45 (0.24)	2.29 (0.32)	14.34 (0.00004)
Parietal_lobe	3.37 (0.19)	2.9 (0.32)	2.65 (0.43)	16.46 (0.00001)
Occipital_lobe	3.15 (0.24)	2.78 (0.29)	2.53 (0.43)	11.2 (0.0002)
Cingulate	3.33 (0.21)	2.85 (0.31)	2.65 (0.35)	17.16 (0.00001)
Cerebellum	2.26 (0.21)	1.88 (0.30)	1.78 (0.29)	12.46 (0.0001)

F-statistic and p-values derived from an ANCOVA across the three groups, with age as a covariate of no interest.

medRxiv preprint doi: https://doi.org/10.1101/2020.01.24.20018697; this version posted January 28, 2020. The copyright holder for this preprint
(which was not certified by peer review) is the author/funder, who has granted medRxiv a license to display the preprint in perpetuity.
It is made available under a CC-BY-NC-ND 4.0 International license .

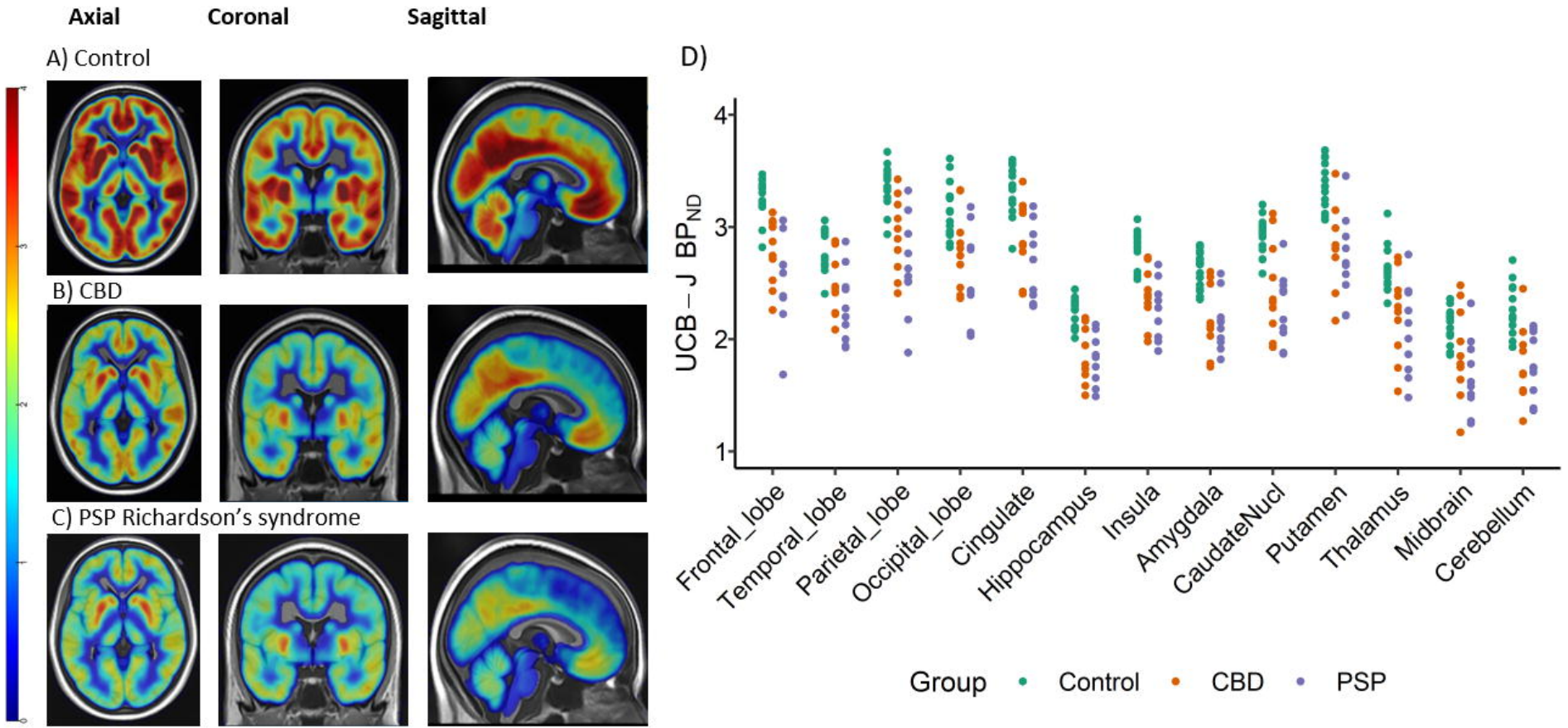
Axial
Coronal
Sagittal
A) Control
B) CBD
C) PSP Richardson's syndrome
D)
UCB – J BP$_{ND}$
4
3
2
1
Frontal_lobe
Temporal_lobe
Parietal_lobe
Occipital_lobe
Cingulate
Hippocampus
Insula
Amygdala
CaudateNucl
Putamen
Thalamus
Midbrain
Cerebellum
Group
Control
CBD
PSP

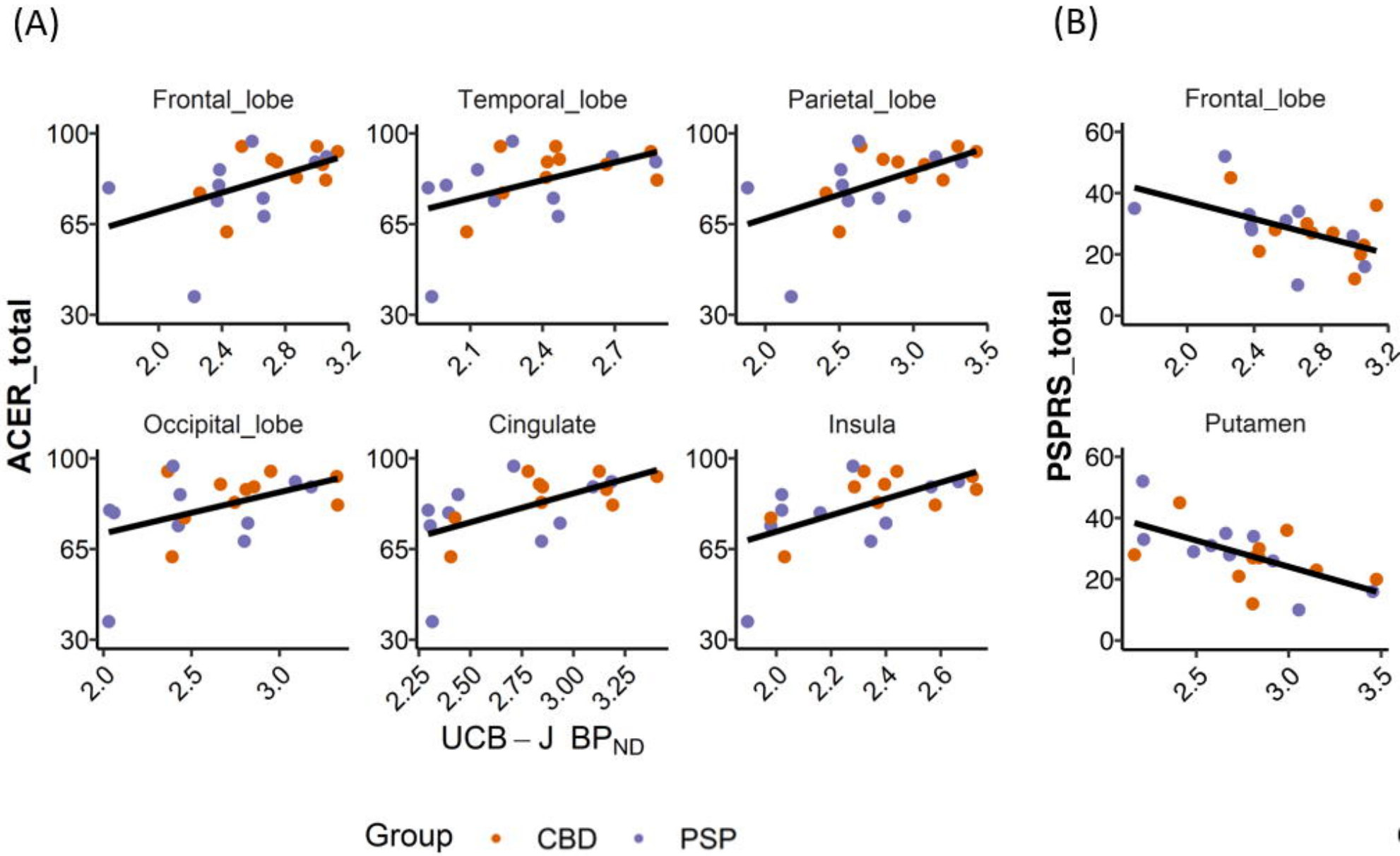
(A)
Frontal_lobe
Temporal_lobe
Parietal_lobe
Occipital_lobe
Cingulate
Insula
ACER_total
UCB – J BP$_{ND}$
(B)
Frontal_lobe
Putamen
PSPRS_total
Group
CBD
PSP